



## RESEARCH ARTICLE

10.1002/2016RS006083

## Special Section:

URSI AT-RASC (Atlantic Radio Science Conference)

## Key Points:

- Digital frequency sweep for spectrum sensing engine
- Measurements of occupancy
- Time variations of spectrum duty cycle

## Correspondence to:

S. Salous,  
sana.salous@durham.ac.uk

## Citation:

Cheema, A. A., and S. Salous (2016), Digital FMCW for ultrawideband spectrum sensing, *Radio Sci.*, 51, 1413–1420, doi:10.1002/2016RS006083.

Received 18 MAY 2016

Accepted 28 JUL 2016

Accepted article online 2 AUG 2016

Published online 25 AUG 2016

## Digital FMCW for ultrawideband spectrum sensing

A. A. Cheema<sup>1</sup> and S. Salous<sup>1</sup><sup>1</sup>School of Engineering and Computing Sciences, Durham University, Durham, UK

**Abstract** An ultrawideband digital frequency-modulated continuous wave sensing engine is proposed as an alternative technique for cognitive radio applications. A dual-band demonstrator capable of sensing 750 MHz bandwidth in 204.8  $\mu$ s is presented. Its performance is illustrated from both bench tests and from real-time measurements of the GSM 900 band and the 2.4 GHz wireless local area network (WLAN) band. The measured sensitivity and noise figure values are  $-90$  dBm for a signal-to-noise ratio margin of at least 10 dB and  $\sim 13$ – $14$  dB, respectively. Data were collected over 24 h and were analyzed by using the energy detection method. The obtained results show the time variability of occupancy, and considerable sections of the spectrum are unoccupied. In addition, unlike the cyclic temporal variations of spectrum occupancy in the GSM 900 band, the detected variations in the 2.4 GHz WLAN band have an impulsive nature.

## 1. Introduction

The ever growing demand of radio spectrum is becoming a challenging task to accommodate in the current frequency allocation scheme. Emerging radio technologies are looking for a few MHz to a few GHz of bandwidth in order to meet consumer demand in cellular, medical, public safety, and local area wireless networks [Jianfeng *et al.*, 2011, Rappaport *et al.*, 2013]. The aim is to provide high data rate services, connectivity, high quality of service, security, and interoperability with the drive to improve the utilization of the radio spectrum in current and upcoming frequency allocation schemes.

To improve spectrum utilization in the current frequency allocation scheme, the unused portions of the radio spectrum (i.e., spectrum holes) can be reutilized. However, to enable this, reliable spectrum occupancy measurements are required to find the spectrum holes in time, frequency, and space. Moreover, these measurements can be beneficial to model the occupancy of the radio spectrum and to define protocols for “when and how” the spectrum holes can be reutilized.

A cognitive radio (CR) is thus an intelligent radio which can learn from the environment and adapt its parameters to provide reliable communication links and improve the spectrum utilization by accessing the unused spectrum opportunistically provided that it is interference free to the licensed users of the network [Haykin, 2005; Tandra *et al.*, 2009; Liu *et al.*, 2013]. To avoid interference to the primary user, a geolocation database can be complemented by a sensing engine (SE) for local monitoring. Thus, a CR device must be able to detect the spectrum holes reliably, which depends on the hardware used to sense the spectrum [Finn *et al.*, 2011] and the detection algorithm [Yucek and Arslan, 2009; De Vito, 2013].

The performance of the SE is measured based on bandwidth, sensitivity, dynamic range, frequency resolution, and sweep time, which is the time to acquire a snapshot of the spectrum [Denkovski *et al.*, 2010; Cabric *et al.*, 2004]. The large sensed bandwidth is required to increase the chances of finding spectrum holes and possible bandwidth aggregation. To detect weak signals, a SE is required to have high sensitivity to overcome the hidden node problem and a large dynamic range for reliable detection of weak signals in the presence of strong signals. A short snapshot time allows the SE to capture short-duration signals, whereas fine resolution bandwidth is needed to capture narrowband signals. For instance, to detect signals in the 2.4 GHz industrial, scientific, and medical (ISM) band the snapshot duration should be on the order of 100–200  $\mu$ s with the narrowest resolution bandwidth being less than 1 MHz [Yuxing *et al.*, 2011].

In this paper in section 2 we discuss the different types of sensing engines and give a summary of the reported measurement parameters. This is followed in section 3 by a description of an ultrawideband (UWB) programmable SE developed for simultaneous measurements in two frequency bands. The measurement setup and data analysis methodology are described in section 4. The results are discussed in section 5 followed by conclusions in section 6.

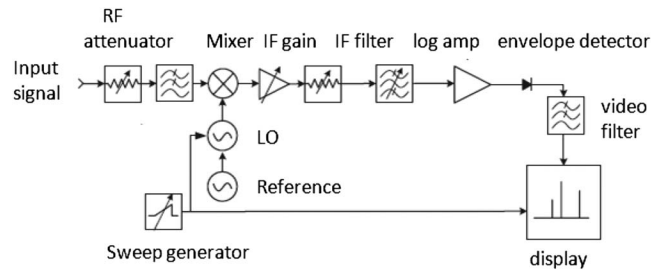


**Figure 1.** Heterodyne sweep method used in spectrum analyzers [Agilent, 2016].

## 2. Approaches of Sensing Engines

Key considerations in the design of spectrum sensing approaches include type of equipment, speed and sophistication of data capture and processing, and degree of integration with software tools for analysis. Energy-based spectrum sensing approaches range from the simple received signal strength indicator to the more sophisticated advanced sensing engines using state of the art radio frequency (RF) and digital techniques [Farrell et al., 2009; Finn et al., 2011]. These sensing solutions can be further categorized as follows:

1. Frequency domain  
 (a) Heterodyne frequency swept method as in traditional spectrum analyzers  
 (b) Frequency swept direct down-conversion  
 2. Time domain direct down-conversion

1. Frequency domain
  - (a) Heterodyne frequency swept method as in traditional spectrum analyzers
  - (b) Frequency swept direct down-conversion
2. Time domain direct down-conversion

The frequency domain method mixes the incoming signal with a frequency sweep across the monitored spectrum [Razavi, 1998]. In traditional spectrum analyzers (SA) the signal is then band-pass filtered at an IF frequency, amplified, and detected by using a log amplifier as shown in Figure 1 [Agilent, 2016]. This approach is commonly called the heterodyne method, and the frequency sweep is normally generated by using analogue frequency generators.

An alternative to the architecture in Figure 1 is the direct down conversion architecture employed in the frequency modulated continuous waveform (FMCW) or chirp sounder as shown in Figure 2 [Salous et al., 1998]. In this technique the received signal is directly mixed down to baseband with a high rate digital frequency sweep. The output is then filtered and digitized for off line analysis by using the double fast Fourier transform (FFT) or processed online with a digital signal processor component if implemented in the hardware.

In the time domain method, the received RF signal is filtered, amplified, and down-converted to baseband by using quadrature demodulation as illustrated in Figure 3 [Razavi, 1998]. The baseband components are then digitized and processed by using digital spectral analysis techniques such as the FFT. Thus, sensing engines based on the direct down conversion technique tend to employ two boards: RF front end and a digital board, which can be interfaced to other boards, thus providing flexibility.

The advantage of the time domain method is its ability to capture the RF bandwidth in a short duration leading to “real-time spectrum analysis”. However, the bandwidth that can be sensed at any instant in time is limited by the sampling rate of the analogue to digital converters (ADC) in the data acquisition unit [Hongjian et al., 2013]. In contrast, the frequency-sweep method results in bandwidth compression which requires a single low rate ADC, which enables large frequency sweeps to be monitored. Comparing the digital frequency swept method with the analogue method, faster sweep rates can be achieved and these in turn enable capturing short duration signals. Current real-time spectrum analyzers have reported bandwidths up to 510 MHz, which enables capturing 3.33 ns pulses [Keysight, 2015].

To study the spectrum utilization, several spectrum occupancy measurements have been performed worldwide in both indoor and outdoor environments by using a variety of sensing engines [Islam et al., 2008; Harrold et al., 2011; Xue et al., 2013; Chiang et al., 2007; Salous, 2010; Qaraqe et al., 2010; Wellens et al., 2007; Lopez-Benitez et al., 2009].

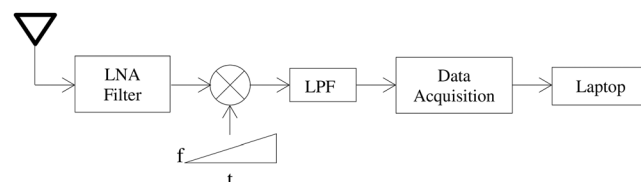


**Figure 2.** Architecture of chirp sounder receiver (swept direct down conversion method).

Table 1 gives a summary of reported measurements which illustrate the trade-off between the type of SE, sensed bandwidth, sensing time, and frequency resolution.

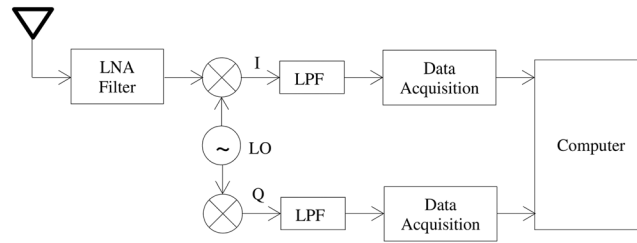


**Figure 3.** (a) Direct quadrature down conversion method.

### 3. Dual Band UWB Sensing Engine

In *Salous* [2010] a wideband SE engine based on Figure 2 was used to capture the UMTS spectrum with a 240 MHz swept bandwidth in 4 ms. To enable measurements of UWB signals, sensing of the TV band (467.25–861.25 MHz) and GSM 900

band, and capturing the 2.4 GHz WLAN signals with short durations, a SE was designed and realized as shown in Figure 4. The SE, which is based on *Salous* [2010], enables high time and frequency resolutions over a larger sensing bandwidth in a shorter sweep duration. The SE consists of four main units: a reference clock distribution unit, a digital frequency sweep (DFS) unit with two frequency ranges of 0.25–1 GHz and 2.2–2.95 GHz, an RF down-converter unit, and a control and command unit.

The reference clock distribution unit contains a 10 MHz clock with frequency multipliers to produce multiple reference clocks for the phase locked loops and for the analogue to digital converter in the command and control unit. The direct digital frequency synthesizer (DDFS) in the DFS unit, clocked at 2.15 GHz, can be programmed via a USB interface to generate a linearly increasing FMCW signal up to 1 GHz. It has a frequency resolution of 0.5006 Hz, and it takes 32 clock cycles to update its frequency. The high frequency components due to the digital to analog conversion process in the DDFS are removed by using a custom deigned low-pass filter (LPF) with a cutoff frequency of 1 GHz as illustrated in Figure 5a before and after filtering. The filtered DDFS output provides the reference signal for the first down-converter to sense radio technologies up to 1 GHz such as TETRA, TV, and the GSM 900 band. The filtered signal is also up converted to 2.2 GHz to 2.95 GHz by using a direct up-converter (UC) with 3.2 GHz local oscillator and a 750 MHz custom designed band-pass filter (BPF) [Feeney and Salous, 2013]. Figure 5b shows the up-converted signal before and after filtering. The down-converter unit has two independent RF chains (RFC), which can provide programmable RF gains up to 30 dB for RFC 1 and 31 dB for RFC 2.

The command and control unit consists of a programmable signal conditioning (SC) circuit, which filters the low IF signal with either a 5 MHz or 10 MHz LPF and provides programmable amplification at baseband up to 43 dB. The received signals are then digitized by a two-channel 14-bit digitizer which supports continuous data transfer rate of 1400 MB/s on a PCI Express Bus. The unit has a field programmable gate array (FPGA) to phase synchronize the digital sweeps of the DDFS and to generate control signals for the RF gains, signal conditioning gains, digitizer, and antenna switching circuit, if required. The logged data can be monitored online or stored for off-line processing where further filtering is applied followed by either a double FFT or a Hilbert transform to compute the received power ( $p_{estimate}^{dBm}$ ). At the beginning of each measurement, the gains are computed based on the sampled data in real time to avoid over driving of the mixers in both of the RF chains or to increase the instantaneous dynamic range (IDR).

The performance of the SE was verified from a number of tests to ensure correct detection. Figure 6 illustrates its detection capability of the 2.4 GHz WLAN signal in the ISM band with a 750 MHz swept bandwidth in a snapshot time of 204.8  $\mu$ s. The continuous wave (CW) signal at 2.3 GHz and the 20 MHz FMCW signal centered

**Table 1.** Summary of Spectrum Occupancy Measurements

Reference	Type of SE	Frequency Range (MHz)	Sensing Bandwidth (MHz)	Sensing Time ( $\mu$ s)	Frequency Resolution (kHz)
Islam <i>et al.</i> [2008]	SA	80–5850	60	828e6	150
Harrold <i>et al.</i> [2011]	SA	300–4900	20	360e6	300
Xue <i>et al.</i> [2013]	SA	450–2700	Variable	42e4	15/100/200
Chiang <i>et al.</i> [2007]	Radio monitoring receiver	806–2750	Variable	(5–10)e6	15/120/250
Salous [2010]	Chirp channel sounder receiver	2000–2400	240	4e3	0.25
Qaraqe <i>et al.</i> [2010]	SA	700–3000	2300	128e3	300
Wellens <i>et al.</i> [2007]	SA	770–5250	1500	1e6	200
Lopez-Benitez <i>et al.</i> [2009]	SA	75–3000	500	(12.5–15)e6	10

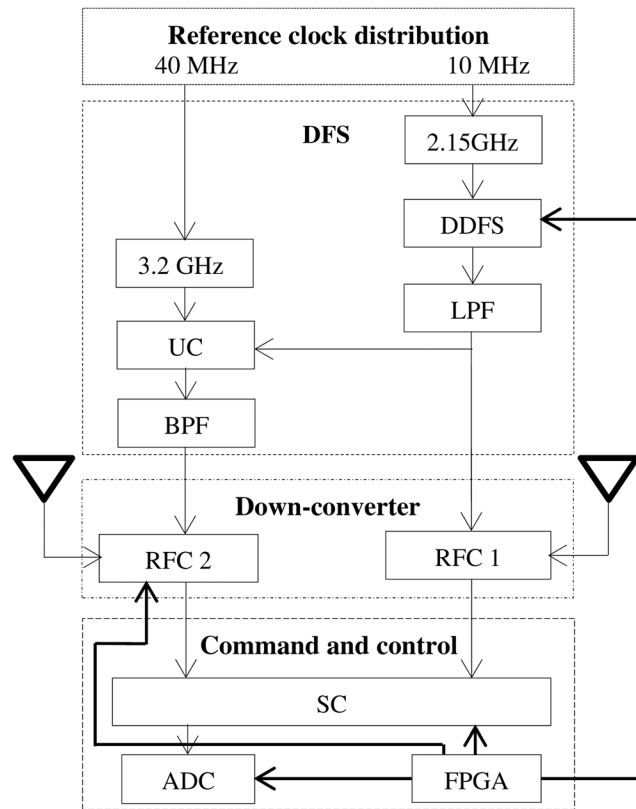


**Figure 4.** Block diagram of proposed SE based on frequency swept direct down-conversion method.

measured at 7 dB for RFC 1 and 4 dB for RFC 2. Table 2 summarizes the measured performance parameters of the developed SE, where the noise figure (NF) is found to be between ~13-14 dB and the measured sensitivity is found to be better than -90 dBm. An IDR value of ~30 dB is achieved in both frequency ranges.

at 2.737 GHz were generated by using signal sources to verify the stability of the SE with time in capturing CW signals and its capability to measure frequency swept signals.

The SE was also calibrated to evaluate its dynamic range and its sensitivity by using a CW signal as the input into the SE. The CW signal was fed via an attenuator, which was gradually increased until the received signal could not be distinguished from the noise floor. The logged data were filtered by using a high-order Gaussian window to obtain a 1 MHz frequency resolution, and the received power ( $P_{receive}^{dBm}$ ) was computed by using the link budget in equation (1):

$$P_{received}^{dBm} = P_{estimate}^{dBm} - RFCgain^{dB} - SCgain^{dB} + losses_{system}^{dB} \quad (1)$$

where  $RFCgain^{dB}$  and  $SCgain^{dB}$  define the gains of the RF and SC gains, respectively. The value of the overall system losses ( $losses_{system}^{dB}$ ) was measured

## 4. Measurements and Data Analysis

### 4.1. Measurements Setup

Measurements were performed in the two frequency bands of the SE at Durham University. The band between 250 MHz and 1 GHz was measured by using a log-periodic antenna placed on top of the roof of the school of engineering and computing sciences and pointing toward the city center as shown in

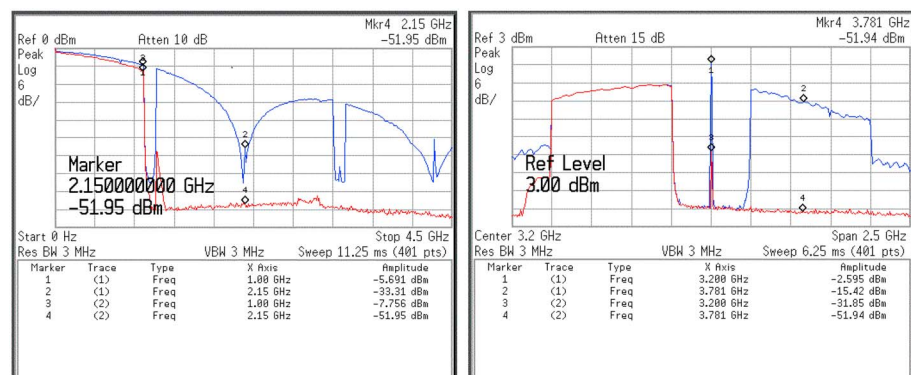


**Figure 5.** (a) Chirp signal before (blue) and after LPF (red). (b) Up-converted signal before (blue) and after BPF (red).

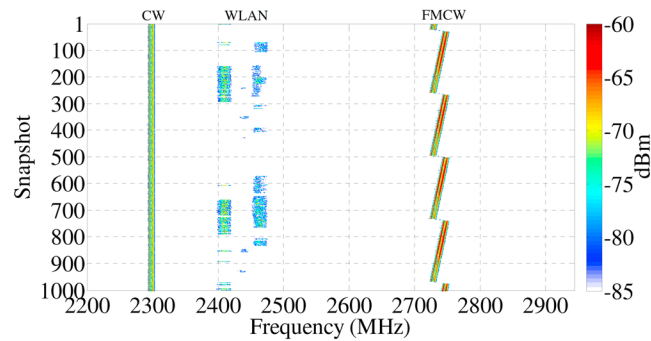


**Figure 6.** Spectrum using the developed SE showing 2.4 GHz WLAN signal, CW signal, and FMCW signal captured with 750 MHz in 204.8  $\mu$ s per snapshot.

Figures 7a and 7b. The measurements were performed with 750 MHz bandwidth swept in 3.2768 ms, and the raw data were processed by using a high-order Gaussian window to obtain a frequency resolution of 200 kHz. The chosen sweep time and frequency resolutions provide a good trade-off to sense signals from various radio technologies. Particularly, it enables the sensing of the GSM 900 signal at the frame level in each channel. (A GSM 900 frame duration is equivalent to 4.615 ms.). Data were

recorded over a 24 h period from 9:30 P.M. (3 July 2014) to 9:30 P.M. (4 July 2014) with 499 sweeps recorded continuously per minute giving a total of 718,560 sweeps.

The band between 2.2 and 2.95 GHz is widely used for the 2.4 GHz WLAN and the LTE 2600 signals. Since the LTE 2600 service is not yet available in Durham city, UK, the SE was configured to 750 MHz bandwidth centered at 2.575 GHz with a time resolution of 204.8  $\mu$ s to ensure packet level detection of the 2.4 GHz WLAN. The measurements were performed by using a discone antenna at 1.5 m above the ground level in an indoor environment as shown in Figure 7.c. Data were collected over a 24 h period in the school of engineering and computing sciences from 1:30 P.M. (15 July 2014) to 1:30 P.M. (16 July 2014) with 2499 sweeps recorded continuously per minute giving a total of 3,598,560 sweeps. The raw data were processed by using a high-order Gaussian window to obtain 1 MHz frequency resolution.

#### 4.2. Data Calibration

The raw data were calibrated for all gains and losses in the system, including cables and antenna, to estimate the received power. To set the threshold level for detection, the noise floor was measured as discussed in section 3 for the exact setups used in the measurements. The detected noise floor was then estimated to be on the order of  $\sim -109$  dBm for the band between 250 MHz to 1 GHz and  $\sim -101$  dBm for the band between 2.2 and 2.95 GHz. The decision thresholds were thus set up for 10 dB signal-to-noise ratio at  $-99$  dBm and  $-91$  dBm, respectively. These values were found empirically by configuring the SE in the respective band and location. The uncertainty in the noise is measured, and 10 dB was found to be the noise free region for occupancy measurements.

#### 4.3. Data Analysis

In cognitive radio, a parameter that can be used to evaluate the availability of the spectrum is the duty cycle, which represents the fraction of time a frequency bin or frequency band is occupied. This is generated first by evaluating the function  $\Omega(t_i, f_j)$  obtained by identifying all the frequency bins  $f_j$ , which are above a certain threshold  $\lambda_j$  chosen to be above the noise floor of the measured power,  $S(t_i, f_j)$ , spectrum for each snapshot,  $t_i$  as in equation (2).

$$\Omega(t_i, f_j) = \begin{cases} 0, & S(t_i, f_j) < \lambda_j \\ 1, & S(t_i, f_j) > \lambda_j \end{cases} \quad (2)$$

**Table 2.** Performance Parameters of Developed SE With 750 MHz Bandwidth

RFC	Centre Frequency (MHz)	Noise Floor (dBm)	NF (dB)	IDR (dB)
1	625	-99.52	14.48	29.89
2	2575	-101.21	12.79	29.98



**Figure 7.** Measurement setups: (a) log periodic antenna for 0.25–1 GHz band, (b) antenna view for 0.25–1 GHz band, and (c) indoor setup on trolley for 2.2–2.95 GHz band.

The duty cycle  $\Psi_j$  can then be estimated for each frequency bin  $f_j$  by finding the average over time as in equation (3), where  $N_t$  is the total number of time observations or snapshots. For a frequency band, the duty cycle  $\Psi$  is found from the average over time and frequency band as in equation (4).

$$\Psi_j = \frac{1}{N_t} \sum_{i=1}^{N_t} \Omega(t_i, f_j) \tag{3}$$

$$\Psi = \frac{1}{N_f} \sum_{j=1}^{N_f} \Psi_j \tag{4}$$

### 5. Results

To estimate the occupancy over the 24 h period, the data were analyzed in two different ways: (1) to identify the received frequency bands by computing the average and maximum values of the power spectrum and (2) to estimate the duty cycle as in equations 2–4. Figures 8a and 8b display the results for the two analysis methods for the frequency range of 250 MHz–1 GHz, respectively. Figure 8a shows that at the measurement location the following subbands were received: subband 1: 250–470 MHz, assigned to military, aeronautical, and public safety radio technologies with the highest power levels detected in the aeronautical services between 450 and 465 MHz; sub band 2: 467–880 MHz, dominated by broadcasting TV transmissions (49 stations separated by 8 MHz) where high-power levels were detected for TV channels 33 (567.25 MHz), 49 (695.25 MHz), 50 (703.25 MHz), 54 (735.25 MHz), 55 (743.25 MHz), 58 (767.25 MHz), and 59 (775.25 MHz) while relatively low-power levels were detected for channels 62 (799.25 MHz) and 63 (807.25 MHz); and subband 3: 0.88–1 GHz used by UHF radio-frequency identification and GSM 900 uplink (890–915 MHz) and downlink (935–960 MHz). The duty cycle in Figure 8b shows that either the transmission is continuously received as for broadcasting TV channel 33 or that the received signal level drops below the threshold such as for TV channel 58 and the GSM 900 downlink signal in non-office hours.

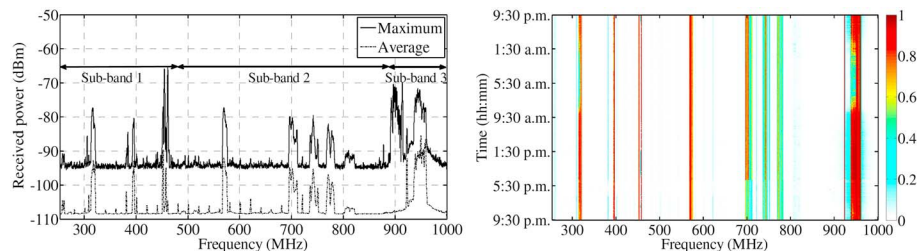


**Figure 8.** (a) Maximum and average power spectrum and (b) 24 h period duty cycle.

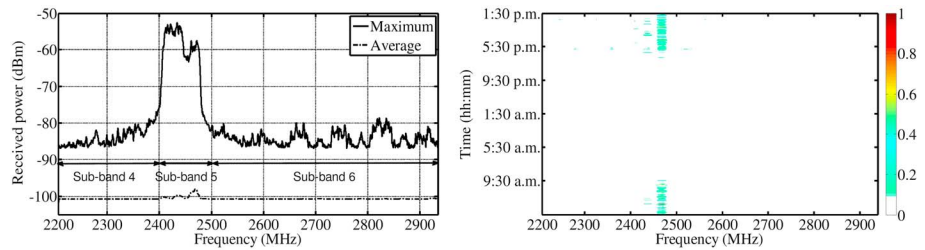


Figure 9. (a) Maximum and average power spectrum and (b) 24 h period duty cycle.

Particularly, multiple 200 kHz narrowband channels were detected in the GSM 900 downlink signal. Similarly, the indoor measurements were processed to estimate the average and maximum spectrum and the duty cycle for the 24 h observation period as illustrated in Figure 9. The frequency range was also divided into three subbands, subband 4: 2200–2400 MHz, subband 5: 2400–2500 MHz, and subband 6: 2500–2950 MHz. Figure 10 displays the utilization of subband 5 which exhibited the highest level of occupancy for a threshold level of  $-91$  dBm. The figure shows that the band is primarily occupied during office hours as it is mainly occupied with the 2.4 GHz WLAN signal.

In the frequency ranges of 2.2–2.4 GHz (subband 4) and 2.5–2.95 GHz (subband 6), no significant activity was recorded, which makes them a suitable choice for CR applications. Table 3 provides a comparison of spectrum utilization among the different subbands. Subband 3 is highly utilized due to the downlink signal of GSM 900. While subbands 1 and 2 are relatively less utilized with spectrum utilization less than 8%. Subbands 4 and 6 have less than 1% spectrum utilization, which is about 625 MHz of unoccupied bandwidth, while subband 5 has spectrum utilization of 3.15%. The overall spectrum utilization in both bands is 8.08%, which indicates that the spectrum is highly underutilized at the measurement location and CR applications can benefit from it by accessing it opportunistically.

The on/off behavior of transmission in the GSM 900 band and the 2.4 GHz WLAN is very important to understand and can be exploited to create spectrum opportunities for CR users, where they can access the frequency bin/channel/band in the time domain [Cheema and Salous, 2014].

### 6. Conclusion

The implementation of a high resolution ultrawideband SE is presented, and its performance is demonstrated. The measured sensitivity is found to be better than  $-90$  dBm with IDR of  $\sim 30$  dB achieved for the full sensing bandwidth.

Measurements taken on the campus of the University over 24 h show that the radio spectrum is highly underutilized and its utilization can be increased by accessing it opportunistically. The spectrum utilization in services like GSM 900 and 2.4 GHz WLAN is relatively high in office hours compared to nonoffice hours. Moreover, due to the ON/OFF behavior of the transmitter in these radio technologies, spectrum holes can be accessed in the time domain. A database of partially occupied or fully unoccupied frequency bins (bands) can be made and shared between CR users for access.

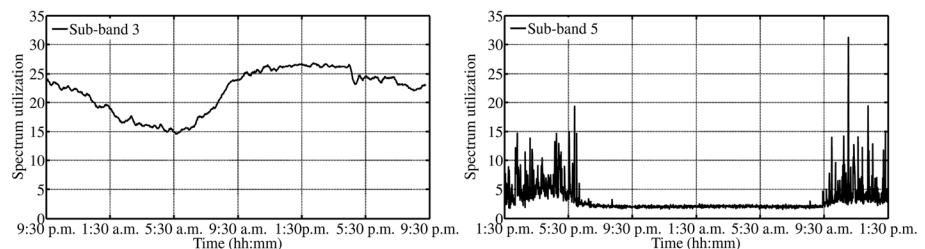


Figure 10. Spectrum utilization over 24 h (a) GSM 900 band and (b) ISM band.

**Table 3.** Comparison of Spectrum Utilization Over 24 H Among Different Bands

Subband	Frequency Range (MHz)	Spectrum Utilization (%)
1	250–470	6.88
2	470–880	7.90
3	880–1000	21.91
4	2200–2400	0.55
5	2400–2500	3.15
6	2500–2950	0.52

### Acknowledgments

The authors would like to thank S.M. Feeney for the design of the analogue circuits in the SE under an EPSRC grant PATRICIAN EP/I00923X/1 and the EU CREW project. Adnan Cheema is funded under a School of Engineering and HMGCC studentship. On request, data supporting conclusions can be obtained.

### References

- Agilent (2016), Spectrum Analysis Basics Application Note 150 Available at. [Available at <http://cp.literature.agilent.com/litweb/pdf/5952-0292.pdf>.]
- Cabric, D., S. M. Mishra, and R. W. Brodersen (2004), Implementation issues in spectrum sensing for cognitive radios. Signals, systems and computers, 2004 Conference Record of the Thirty-Eighth Asilomar Conference on, 7–10 Nov. 2004. 772–776.
- Cheema, A. A., and S. Salous (2014), High resolution temporal occupancy measurements to characterize idle time window in ISM band General Assembly and Scientific Symposium (URSI GASS), 2014 XXXIth URSI, 16–23 Aug. 2014. 1–4.
- Chiang, R. I. C., G. B. Rowe, and K. W. Sowerby (2007), A quantitative analysis of spectral occupancy measurements for cognitive radio Vehicular Technology Conference, 2007. VTC2007-Spring. IEEE 65th, 22–25 April 2007. 3016–3020.
- De Vito, L. (2013), Methods and technologies for wideband spectrum sensing, *Measurement*, 46, 3153–3165.
- Denkovski, D., M. Pavloski, V. Atanasovski, and L. Gavrilovska (2010) Applied Sciences in Biomedical and Communication Technologies (ISABEL), 2010 3rd International Symposium on, 7–10 Nov. 2010. 1–5.
- Farrell, R., M. Sanchez, and G. Corley (2009), Software-defined radio demonstrators: An example and future trends, *Int J Digit Multimedia Broadcasting*, 2009, 12.
- Feeney, S. M., and S. Salous (2013), High order micro-strip filters to support signal generation and translation Passive RF and Microwave Components, 4th Annual Seminar on, 18–18 March 2013. 1–3.
- Finn, D., et al. (2011), Experimental assessment of tradeoffs among spectrum sensing platforms, in *Proceedings of the 6th ACM International Workshop on Wireless Network Testbeds, Experimental Evaluation and Characterization (WINTECH '11)*, pp. 67–74, ACM, New York, doi:10.1145/2030718.2030733.
- Harrold, T., R. Cepeda, and M. Beach (2011), Long-term measurements of spectrum occupancy characteristics New Frontiers in Dynamic Spectrum Access Networks (DySPAN), 2011 IEEE Symposium on, 3–6 May 2011. 83–89.
- Haykin, S. (2005), Cognitive radio: Brain-empowered wireless communications, *Selected Areas in Commun, IEEE J on*, 23, 201–220.
- Hongjian, S., A. Nallanathan, W. Cheng-Xiang, and C. Yunfei (2013), Wideband spectrum sensing for cognitive radio networks: A survey, *Wireless Commun, IEEE*, 20, 74–81.
- Islam, M. H., et al. (2008), Spectrum survey in Singapore: Occupancy measurements and analyses Cognitive Radio Oriented Wireless Networks and Communications, 2008. CrownCom 2008. 3rd International Conference on, 15–17 May 2008. 1–7.
- Jianfeng, W., M. Ghosh, and K. Challapali (2011), Emerging cognitive radio applications: A survey, *Commun Mag, IEEE*, 49, 74–81.
- Keysight (2015), Real-time spectrum analyzer Available at. [Available at <http://www.keysight.com/en/pc-2278039/real-time-spectrum-analyzer-rtsa?cc=US&lc=eng>.]
- Liu, X., G. Bi, M. Jia, Y. L. Guan, W. Zhong, and R. Lin (2013), Joint optimization of sensing threshold and transmission power in wideband cognitive radio with energy detection, *Radio Sci.*, 48, 359–370. doi:10.1029/2012RS005009.
- Lopez-Benitez, M., A. Umberto, and F. Casadevall (2009), Evaluation of spectrum occupancy in Spain for cognitive radio Applications Vehicular Technology Conference, 2009. VTC Spring 2009. IEEE 69th, 26–29 April 2009. 1–5.
- Qaraqe, K. A., H. Celebi, M. S. Alouini, A. El-Saigh, L. Abuhantash, M. Al-Mulla, O. Al-Mulla, A. Jolo, and A. Ahmed (2010), Measurement analysis of wideband spectrum utilization in indoor outdoor environments *International Conference on Communications Technologies (ICCT 2010)*.
- Rappaport, T. S., S. Shu, R. Mayzus, Z. Hang, Y. Azar, K. Wang, G. N. Wong, J. K. Schulz, M. Samimi, and F. Gutierrez (2013), Millimeter wave mobile communications for 5G cellular: It will work!, *Access, IEEE*, 1, 335–349.
- Razavi, B. (1998), *RF Microelectronics*, Prentice-Hall, Englewood Cliffs, N. J.
- Salous, S. (2010), Chirp sounder measurements for broadband wireless networks and cognitive radio Communication Systems Networks and Digital Signal Processing (CSNDSP), 2010 7th International Symposium on, 21–23 July 2010. 846–851.
- Salous, S., N. Niikandro, and N. F. Bajji (1998), Digital techniques for mobile radio chirp sounders, *Proceedings - Commun, IEE*, 145, 191–196.
- Tandra, R., S. M. Mishra, and A. Sahai (2009), What is a spectrum hole and what does it take to recognize one? *Proc. IEEE*, 97, 824–848.
- Wellens, M., J. Wu, and P. Mahonen (2007), Evaluation of spectrum occupancy in indoor and outdoor scenario in the context of cognitive radio Cognitive Radio Oriented Wireless Networks and Communications, 2007. CrownCom 2007. 2nd International Conference on, 1–3 Aug. 2007. 420–427.
- Xue, J., Z. Feng, and P. Zhang (2013), Spectrum occupancy measurements and analysis in Beijing, *IERI Procedia*, 4, 295–302.
- Yucek, T., and H. Arslan (2009), A survey of spectrum sensing algorithms for cognitive radio applications, *Commun Surv Tutorials, IEEE*, 11, 116–130.
- Yuxing, H., W. Jiangtao, D. Cabric, and J. D. Villaseñor (2011), Probabilistic estimation of the number of frequency-hopping transmitters, *Wireless Commun, IEEE Trans on*, 10, 3232–3240.